ORAL/POSTER Reference: ICF 100292PR

THE ROLE OF CONSTRAINT IN MIXED MODE I AND II DUCTILE FRACTURE

T.D. Swankie[1], and D.J. Smith[2]

1. Structural Integrity Technology Group, TWI Ltd., Cambridge, CB1 6AL, UK
2. Department of Mechanical Engineering, University of Bristol, Bristol, BS8 1TR, UK

ABSTRACT

There is a wealth of experimental data that demonstrates that the resistance to mode I ductile tearing is dependent on specimen dimensions and crack depth. For mode II there is significantly less data. In this paper, the results of a series of mode II and mixed mode I and II experiments, using A508 Class 3 ferritic steel at ambient temperature, are summarised. Tests were carried out using single edge notched specimens and a special fixture. As expected for mode I loading, specimens with low constraint resulted in high resistance to tearing. In contrast, for mode II the tearing resistance was lower than for fully constrained mode I and was not influenced by specimen constraint. For mixed mode loading, the transition from mode I to mode II was a strong function of constraint. In some specimens, additional shear reduced constraint, but in other specimens of different dimensions additional shear led to lower tearing resistance.

KEYWORDS

Mixed mode, steel, ductile, R-curve, constraint

INTRODUCTION

More recently there have been extensive studies [1-3] on the mixed mode ductile fracture of steels in an attempt to provide information for assessing the integrity of real components. However, the method for inferring the integrity of real components is uncertain. This is because the behaviour of laboratory test specimens is known to be dependent on specimen size. For example, in mode I many results [4,5] have demonstrated that ductile fracture toughness varies considerably when the crack length remains the same and the specimen dimensions are changed. The general approach for mode I loading is to consider the effects of specimen dimensions and geometry through a measure of crack tip constraint. Two parameter methods such as K-T [6] and J-Q [7] have been developed, where the second terms provide a measure of constraint. In this paper a summary of the results of an experimental study [1] are provided. The aim is to obtain an understanding of the role of shear and constraint in ductile fracture for combinations of tension (mode I) and shear (mode II) loading on a ferritic steel.

EXPERIMENTAL METHODS

Material and specimens

The material for the experiments was A508 Class 3 steel. The chemical composition, in wt% is; 0.16 C, 1.34 Mn, 0.007 S, 0.004 P, 0.22 Si, 0.67 Ni, 0.17 Cr, 0.51 Mo, 0.06 Cu, 0.004 Sb, 0.01 Al, 0.004 Sn, 0.019 As, <0.01V, <0.01 Ti and <0.01 Nb. The S-L orientation was chosen for the fracture tests since earlier studies [2] identified this as the least tough orientation. The basic tensile properties at ambient temperature are 430 MPa, 561 MPa and 201 GPa, yield and tensile strength, and elastic modulus respectively.

Plain sided, single edge notch (SEN) specimens were used. The specimen thickness B was varied from 10 to 40mm and width W from 20 to 80mm. The normalised crack depth, a_o/W ratio was 0.5 for all tests. In each test the load was applied directly through the crack tip.

Test Fixture and Procedure

Mixed mode I/II loading was applied using a test fixture (Fig.1) clamped around the SEN specimen, similar to that designed by Davenport [2]. The fixture is described in detail elsewhere [1]. All fracture tests were carried out in air at ambient temperature in a servohydraulic test machine. The tests were done under displacement control at a constant rate of approximately 0.5mm/min.

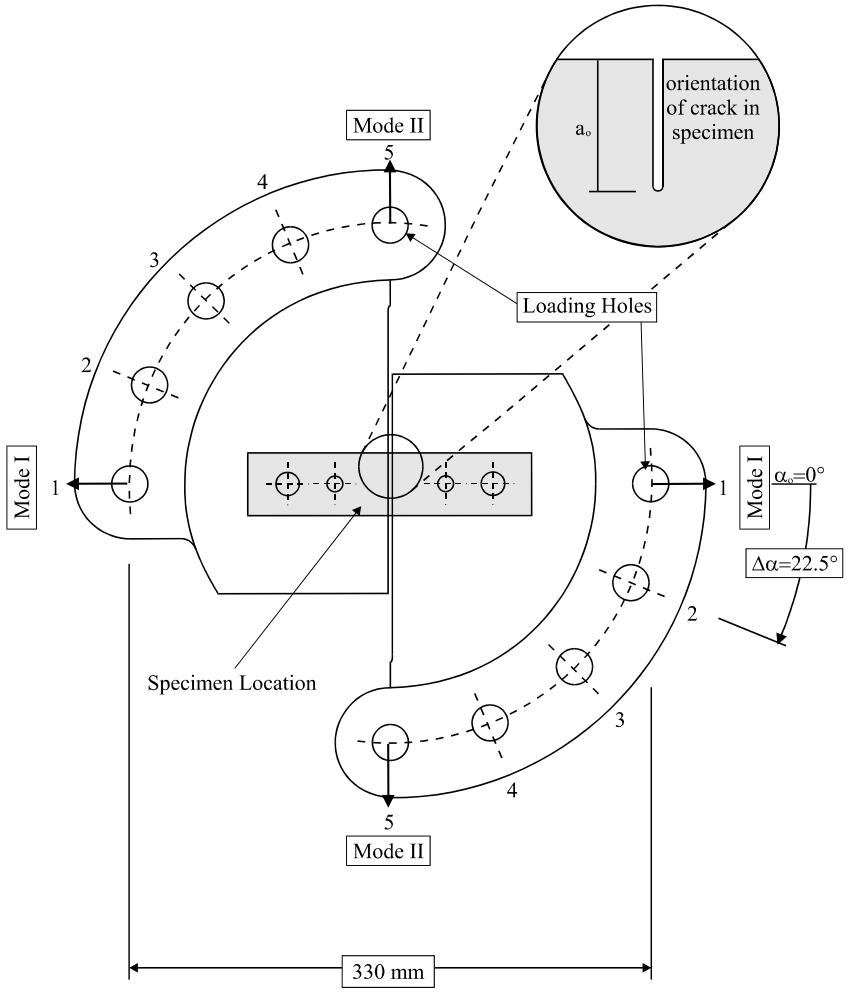

Fig.1. Layout of mixed mode test fixture

The elastic-plastic fracture toughness was calculated in terms of J from the area beneath the loading portion of the applied load versus load line displacement curve [8]. For a given mixed mode loading angle α (see Fig.1), J was calculated using,

$$J_T = \frac{P_{\max}^2\left(1-\nu^2\right)\left\{f\left(\frac{a_o}{W}\right)_I^2 + f\left(\frac{a_o}{W}\right)_{II}^2\right\}}{B^2WE}\left\{1-\frac{\eta_p}{\eta_e}\right\} + \frac{\eta_p}{B\left(W-a_o\right)}\left\{U_T - \frac{P_{\max}^2}{2k}\right\} \quad (1)$$

where P_{max} refers to maximum load, $f(a_o/W)$ and η are geometry dependant functions, U is the plastic energy and k is a machine stiffness function. Values of $f(a_o/W)$ and η were calculated from plane strain finite element studies, using ABAQUS, and values of k for a given α were determined experimentally. The subscripts I and II refer to mode I and mode II respectively, and e and p denote elastic and plastic respectively.

RESULTS

A total of 109 specimens of varying thickness, B (10mm, 20mm and 40mm) and width, W (20mm, 40mm and 80mm) were tested; 32 specimens in mode I (α=0.0°), 35 in mode II (α=90.0°), and 42 in mixed mode loading (11 at α=22.5°, 19 at α=45.0° and 12 at α=67.5°). From each set of tests (corresponding to a particular size of specimen) multi-specimen crack growth resistance curves (R-curves) were generated using the following power law expression,

$$J = C_1\left(\Delta a\right)^{C_2} \quad (2)$$

where, Δa is the increment of crack growth, and C_1 and C_2 are curve fitting parameters which were derived from an initial first order fit of all applicable data for a specific specimen size and mode of loading.

The R-curves for mode I loading are shown in Fig.2. As can be seen, for W=20mm specimens tested in mode I, the effect of thickness (10mm≤B≤40mm) on crack initiation toughness, J_{init}, measured at Δa=0.2mm, and tearing resistance (measured by the slope of the R-curve, dJ/da) was negligible. However, J_{init} and dJ/da decreased significantly as W increased for a given B.

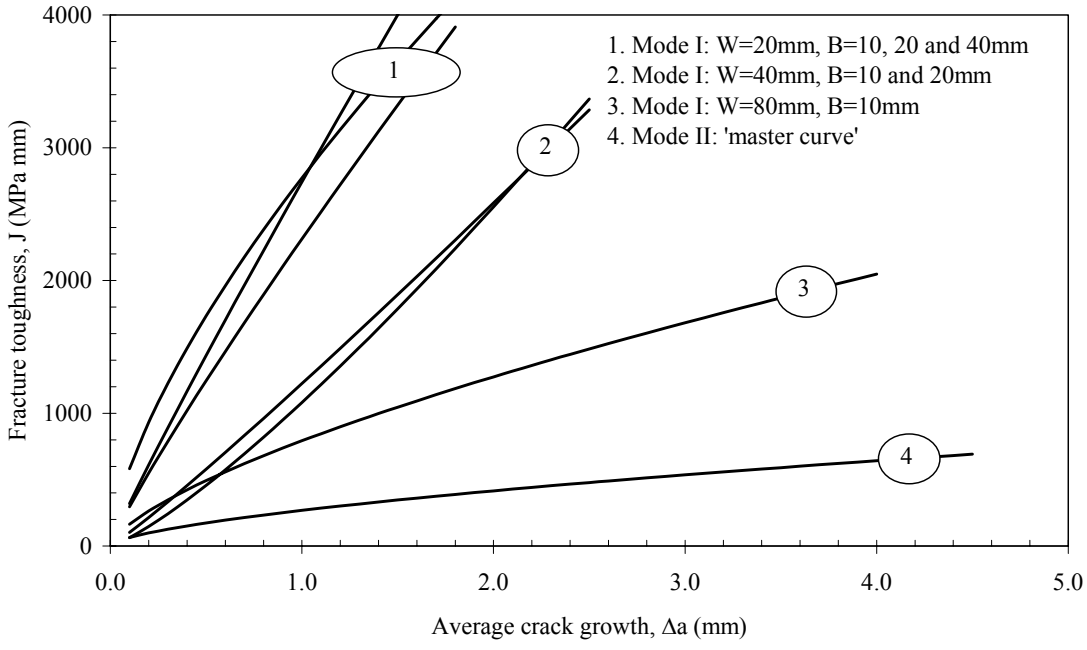

Fig.2 mode I and mode II R-curves: effect of specimen size

All mode II data, regardless of specimen size, can be described by a single curve (a 'master curve'), thus suggesting that the ductile tearing resistance for mode II loading is size independent. The mode II master curve is also shown in Fig.2. Both J_{init} and dJ/da were lower for mode II loading than for mode I.

To investigate the effect of mixed mode loading, 10mm thick specimens were used. This is because the range of specimen thickness tested in both mode I and mode II demonstrated that thickness effects were negligible, in terms of J_{init} and dJ/da. For each combination of tensile and shear loading (α=22.5°, 45.0° and 67.5°), specimens with W=20mm, 40mm and 80mm were tested. An additional 4 tests were done for α=45.0° on B=40mm specimens (W=20mm), to establish whether the negligible effect of thickness seen in the pure mode studies could be confirmed.

R-curves for a given B and W are shown in Fig.3 (B=10mm, W=20mm) and Fig.4 (B=10mm, W=80mm) for different combinations of tension and shear. For B=10mm, W=20mm (see Fig.3) the R-curves steadily decrease with increasing mode II. However, at Δa=0.2mm, J_{init} for mode I loading is similar to J_{init} for α=45.0°. For B=10mm, W=80mm (see Fig.4) the R-curve for mode I loading lies between the R-curves for α=45.0° and 67.5°. At Δa=0.2mm, J_{init} for mode I loading is similar to J_{init} for α=67.5°. The R-curve for α=22.5° is the highest and with increasing mode II the R-curves steadily decrease. Although not shown, the R-curves for B=10mm, W=40mm also decrease with increasing mode II, and at Δa=0.2mm, J_{init} for mode I loading is similar to J_{init} for mode II.

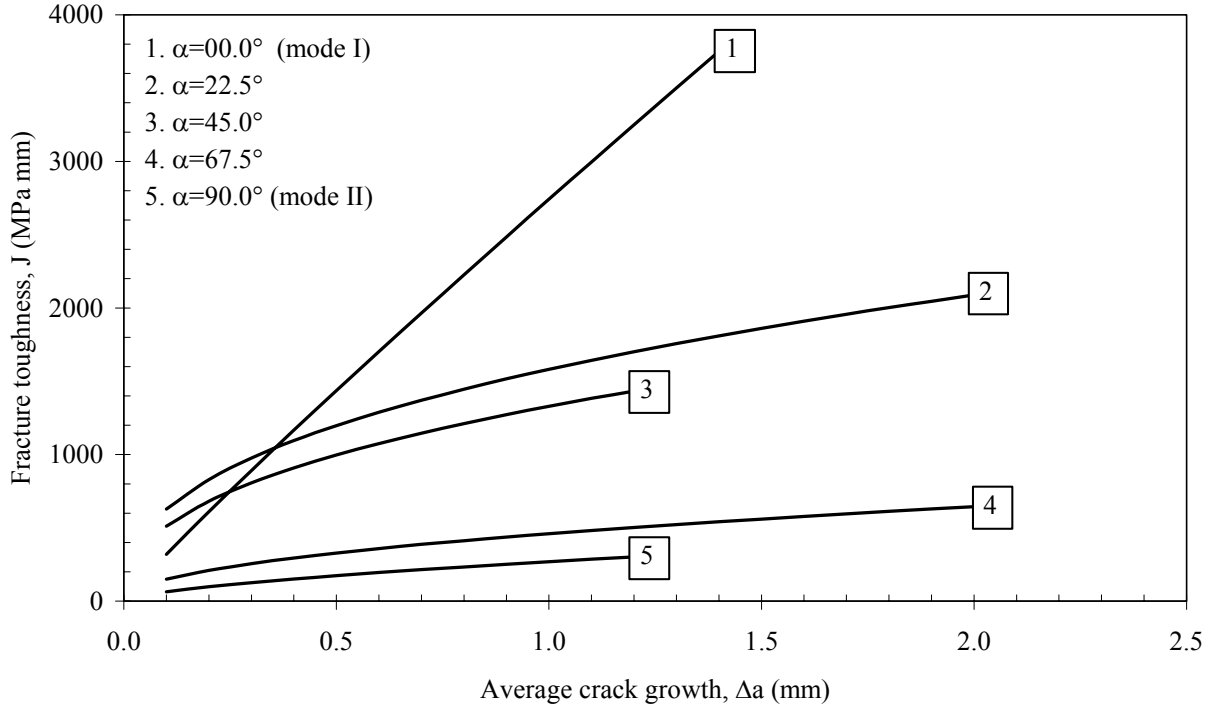

Fig.3 Mixed mode I/II R-curves: W=20mm, B=10mm

DISCUSSION

Initial studies have investigated the effect of specimen size when the crack tip is subject to conditions of pure mode I loading for a crack depth ratio, a_o/W of 0.5. The experiments demonstrate that an increase in specimen thickness has a negligible effect on J_{init} and dJ/da in mode I (see Fig.2). This is in agreement with Joyce and Link [5] who tested HSLA HY100 using SEN specimens up to 50mm thick. In contrast a number of investigators, also examining C-Mn steels [9-11], have found that an increase in specimen thickness causes dJ/da to decrease but the reported effects on J_{init} are varied.

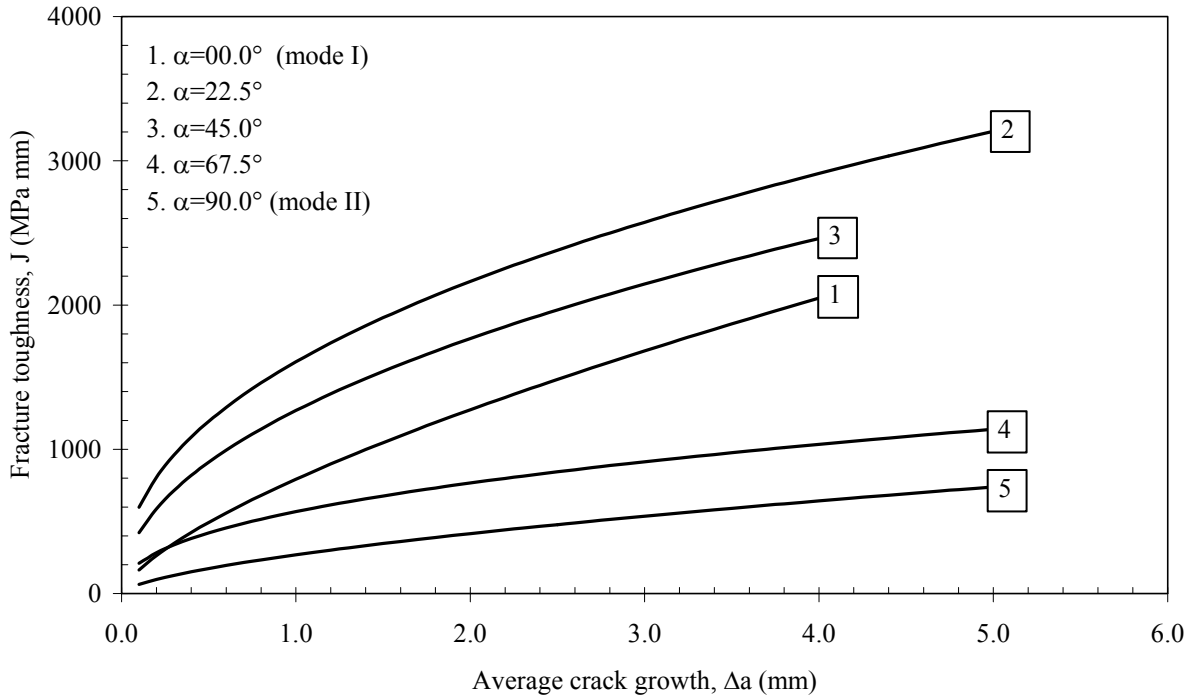

Fig.4 Mixed mode I/II R-curves: W=80mm, B=10mm

The effect of the variation in specimen width is also shown in Fig.2. Width has a significant effect on both J_{init} and dJ/da since J_{init} for W=20mm is greater than for W=80mm (which is similar to W=40mm), and dJ/da for W=20mm is greater than for W=80mm (which is less than for W=40mm).

The mode II experiments demonstrate that specimen size has a negligible effect on J_{init} and dJ/da, and microscopic examination has shown that failure is due to shear localisation. Unlike mode I, at the onset of shear loading asymmetric blunting of the notch tip causes one side to blunt and the other to sharpen. Similar features have been observed by Aoki et al. [12] who demonstrated that the strain and void volume fraction were higher at the sharpened corner with increasing load due to the distribution of equivalent plastic strain. In the present experiments a higher density of microvoids nucleated at the sharpened corner where the localisation of plastic strain was high. This led to a loss in stress carrying capability and subsequent failure of the ligament between neighbouring voids by a localised shear mechanism.

Mixed mode loading causes asymmetric blunting of the crack tip where the angle of the blunted tip, caused by the forward rotation of the upper crack flank in relation to the lower, corresponds approximately to the mixed mode loading angle, α. For α=45.0° and 67.5°, shear cracks initiated at the blunt side of the deformed notch. In contrast, competing failure mechanisms were observed for loading through α=22.5°. This was due to the variation in specimen width causing a change in constraint such that the wider specimens (W=80mm) failed in a manner similar to that observed in mode I while the smaller width specimens (W=20mm) failed by shear localisation.

Figure 3 (W=20mm) shows a proportional decrease in both J_{init} and dJ/da with increasing mode II until the limiting condition of pure mode II is reached. With the exception of the mode I R-curve, the R-curves for W=80mm also follow this trend as shown in Fig.4. However, the mode I R-curve is no longer an upper bound curve. The increase in constraint associated with an increase in specimen width is reflected only in the mode I R-curve and not when a component of mode II is present. The mode I R-curves suggest that in addition to tensile loading at the crack tip, a proportion of this load is attributed to bending. Bend loading

is not reflected in the curve for W=20mm but becomes increasingly effective as W increases. The mixed mode R-curves for W=40mm show a similar trend to those for W=80mm, although the decrease in dJ/da is not as great.

CONCLUSIONS

1. Mode II resistance to ductile tearing for A508 Class3 steel was found to be independent of specimen size and can be characterised by a "master-curve". The mode II master curve was lower than the mode I R-curve for high constraint.
2. For mode I loading there was an increase in constraint with increasing specimen width in mode I loading such that the slope of the R-curve decreased. The effect of increasing specimen thickness was negligible.
3. For some mixed mode loading conditions and larger specimen sizes, the application of shear loading decreased constraint and increased the resistance to ductile tearing.
4. For smaller specimens subjected to mixed mode loading, there was a proportional decrease in tearing resistance from mode I to mode II with an increase in shear loading.

ACKNOWLEDGEMENTS

The authors would like to acknowledge the financial support given by the Engineering and Physical Science Research Council (EPSRC) and British Energy Group plc

REFERENCES

1. Swankie, T.D. (1999). PhD Thesis, University of Bristol, UK.
2. Davenport, J.C.W. (1993). PhD Thesis, University of Bristol, UK.
3. Laukkanen, A., Wallin, K., and Rinitimaa, R. (1999) In *Mixed-Mode Crack Behaviour*, ASTM STP 1359
4. Gibson, G.P., Druce, S.G., and Turner, C.E. (1987). *International Journal of Fracture*, 32, pp.219-240
5. Joyce, J.A. and Link, R.E. (1995). In *Fracture Mechanics: Twenty-sixth Volume*, ASTM STP 1256,142-177
6. Betegon and Hancock (1991), *Journal of Applied Mechanics*, 58, 104-110
7. O'Dowd and Shih (1992), *Journal of the Mechanics and Physics of Solids*, 40, 989-1015
8. Sumpter, J.D.G. and Turner, C.E. (1976) In *Cracks and Fracture*, ASTM STP 601, 3-18
9. Andrews, W.R. and Shih, C.F. (1979). In *Elastic-Plastic Fracture*, ASTM STP 668, 426-450
10. G.P. Gibson, G.P (1986), In *Size Effects in Fracture*, I.Mech.E., 33-36
11. Turner, C.E. (1986) In *Size Effects in Fracture*, I.MechE., 25-32
12. Aoki, S., Kishimoto, K., Yoshida, T. and Sakata, M. (1987*), Journal of the Mechanics and Physics of Solids*, 35, 431-455